

The preliminary indicated level of hydrogen is higher, by a little more than 1 order of magnitude than that of helium, but higher by approximately 3 orders of magnitude than the levels of neon and argon. Nearly all the hydrogen evolved is driven off by the time a temperature of 800°C is reached, whereas heavier gases continue to evolve in significant amounts to higher temperatures, owing to their slower diffusion from the bulk of the solid.

Results of thermogravimetric analysis show that, unless oxygen-bearing impurities are held to very low levels during heating in the range 600° to 1200°C, net weight gains of the sample can actually occur while the hydrogen, nitrogen, inert gases, and other contaminants are still evolving. This indicates that the lunar dust is received in a not fully oxidized state. This result is compatible with the observation of free, nonmeteoritic iron discussed above, and with some of the other phases observed.

The heating of the fines in high-purity helium reproducibly produced melting, with some gas evolution, at a temperature of approximately 1165°C. Upon cooling this produced the characteristic porous, dark glassy phase observed abundantly in some of the received samples. Thus it is clear that melting of the powder, probably by meteoritic impact, is the cause of this structural feature, but that temperatures well over 1100°C are required.

R. L. FLEISCHER, E. L. HAINES*

R. E. HANNEMAN, H. R. HART, JR.

J. S. KASPER, E. LIFSHIN

R. T. WOODS

General Electric Research
and Development Center, Schenectady,
New York 12301

P. B. PRICE

University of California, Berkeley

References and Notes

1. R. L. Fleischer, P. B. Price, R. M. Walker, *Annu. Rev. Nucl. Sci.* 15, 1 (1965); *Science* 165, 383 (1965).
2. R. L. Fleischer and P. B. Price, *J. Geophys. Res.* 69, 331 (1964); *Geochim. Cosmochim. Acta* 28, 755 (1964).
3. R. L. Fleischer, P. B. Price, R. M. Walker, M. Maurette, *J. Geophys. Res.* 72, 331 (1967).
4. R. M. Walker, *Proceedings Clermont-Ferrand Track Conference* (1969), vol. 2 p. VII-2.
5. R. L. Fleischer, P. B. Price, R. M. Walker, M. Maurette, G. Morgan, *J. Geophys. Res.* 72, 355 (1967).
6. R. L. Fleischer, P. B. Price, R. M. Walker, *ibid.* 70, 2703 (1965); *Geochim. Cosmochim. Acta* 32, 21 (1968).
7. D. Lal and R. S. Rajan, *Nature* 223, 269 (1969); P. Pellas, G. Poupeau, J. C. Lorin, H. Reeves, J. Audouze, *ibid.*, p. 272.
8. W. H. Huang and R. M. Walker, *Science* 155, 1103 (1967).
9. L. H. Aller, *Stars and Stellar Systems*: vol 6, *Stellar Atmospheres*, G. P. Kuiper, Ed.

(Univ. of Chicago Press, Chicago, 1960), p. 156.

10. Lunar Sample Preliminary Examination Team, *Science* 165, 1211 (1969).

11. We acknowledge the able experimental assistance of R. B. Bolon, H. C. Couch, W. R. Giard, A. S. Holik, E. F. Koch, L. Osika, G. P. Schacher, and C. Van Buren. Samples of rock 17 were taken with the cooperation and help of J. R. Arnold, D. Lal, M. Maur-

ette, and R. M. Walker. Proton irradiations at the Princeton-Pennsylvania accelerator were carried out with the aid and cooperation of H. Allen and F. Homan. This work was supported in part by NASA under contract NAS 9-7898.

* Permanent address: Jet Propulsion Laboratory, Pasadena, California.

4 January 1970

Rare Gases in Lunar Samples: Study of Distribution and Variations by a Microprobe Technique

Abstract. *The rare gas distribution in lunar soil, breccias, and rocks was studied with a micro-helium-probe. Gases are concentrated in grain surfaces and originate from solar wind. Helium-4 concentrations of different mineral components vary by more than a factor of 10 apart from individual fluctuations for each type. Also grains with no detectable helium-4 exist. Titanium-rich components have the highest, calcium-rich minerals the lowest concentrations. The solar wind was redistributed by diffusion. Mean gas layer thicknesses are 10, 6, and 5 μm for helium, neon, and argon respectively. Lithic fragments in breccias contain no solar gases. Glass pitted surfaces of crystalline rocks contain about 10⁻² cubic centimeter of helium-4 per square centimeter. Etched dust grains clearly show spallogenic and radiogenic components. The apparent mean exposure age of dust is approximately 500 × 10⁶ years, its potassium-argon age is approximately 3.5 × 10⁹ years. Cavities of crystalline rocks contain helium-4, radiogenic argon, H₂, and N₂.*

One of the first important observations of the Preliminary Examination Team (1) was the occurrence of large amounts of He, Ne, and Ar in lunar fines and breccias. Their relative abundances and the isotopic composition resemble the solar abundances as well as the abundances of light primordial rare gases. The gases could be due to trapped solar wind, to trapped primordial gases, or to stopped solar flare particles. The distribution of these gases on a microscale provides the clue to their origin. Enrichment* at the surface of grains points to solar wind, whereas a homogeneous distribution is expected for solar flare particles or for primordial gases. Diffusive fractionation

of light and heavy rare gases yields information about the thermal history of lunar samples and about turnover rates. A split of the components could yield cosmic ray exposure ages and radiogenic ages. Also, the original orientation of rock surfaces can be inferred from gas concentration profiles.

The combination of a microprobe with a He mass spectrometer has previously been applied to gas-rich meteorites (2). Samples are bombarded by a 35 keV electron beam of 1 μA with a beam width of ~ 10 μm. Helium-4 in situ liberated by the electron beam was registered by a 60° mass spectrometer simultaneously with elements like Ti, Fe, Ca, Cr, and Mn. Helium profiles

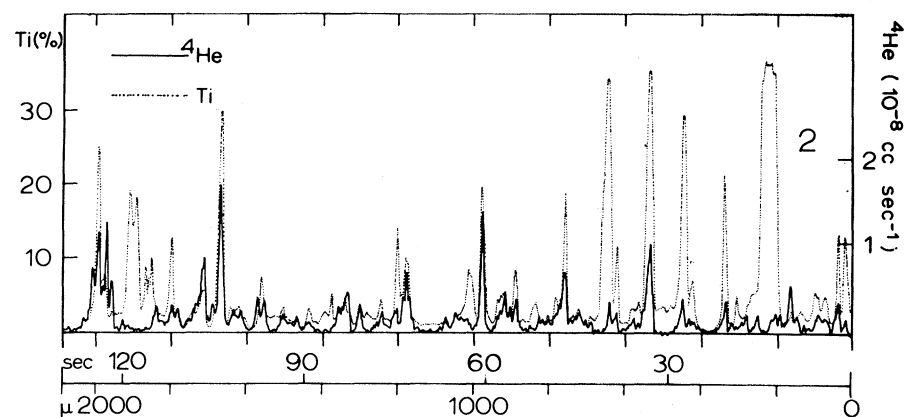


Fig. 1. Correlation of ⁴He and Ti in lunar breccia 10019.13.

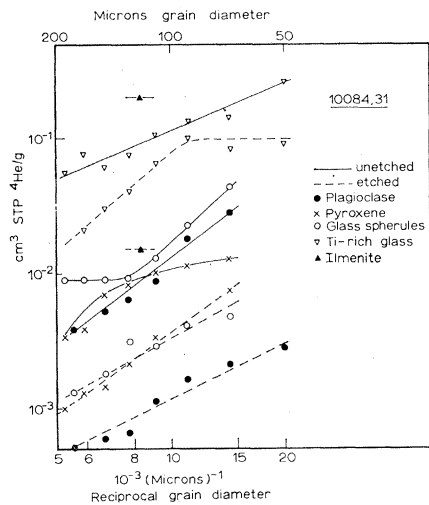


Fig. 2. Average ^4He concentrations plotted against reciprocal diameter of 800 hand-picked dust particles before and after etching.

related to the variation of these elements were obtained. The sample holder was provided with a hat to yield efficient gas collection, with a resulting sensitivity of $\sim 10^{-8}$ cm^3 of ^4He per millivolt per second. Calibration was made by means of a standard leak and by comparison with statically measured test samples. The technique has been applied in a scanning mode (16 $\mu\text{m}/\text{sec}$) to polished breccias and rocks as well as to surfaces of unpolished rocks. A special mechanism kept the beam in focus even for irregularly shaped samples. The high gas retentivity of the minerals required a larger beam, which in turn caused a larger beam diameter. Therefore the local resolution was sometimes less than the average grain diameter. Hence, to supplement the helium profiles with data about well defined minerals, 800 handpicked grains of five major constituents of lunar dust and of different grain sizes were singly analyzed. Half the 800 grains were etched with a $\text{HF}/\text{H}_2\text{SO}_4$ mixture to remove the outer 2 μm of each grain. Etching velocities were determined under the microscope. Etching times varied between 8 seconds (glassy fragments) and 2 minutes (ilmenite). All grains were singly mounted and bombarded with the electron beam, and ^4He was analyzed together with Ti or Fe. Each grain was degassed by a single shot. During bombardment, the irregularly shaped crystals were melted to spherules. From their diameters, precise volumes were determined under the microscope. To supplement the results and to check the calibration of the dy-

namic measurements, seven grain size fractions of unseparated lunar dust were analyzed for He, Ne, and Ar in a static mass spectrometer. Also, an etched portion (adjusted to etch 2 μm of the pyroxene) was measured.

To analyze gases included in cavities of crystalline rocks, chips were broken in the high vacuum system without heating. Non-noble gases were rapidly scanned with a mass filter, rare gases were measured mass spectrometrically.

A ^4He -Ti scan typical for breccias is shown in Fig. 1. It reveals a very inhomogeneous He distribution. Helium is concentrated in spots of some 10 μm in diameter, mostly in very fine grained areas; larger grains and especially small crystalline inclusions are poor in ^4He . A strong correlation between Ti content and He is found. The content of Fe, Cr, and Mn is also correlated with He, but to a lesser extent and mostly involving Fe. On the other hand, Ca and He are inversely related. These findings can be generalized from hundreds of scans across breccias 10019.13, 10046.19 and 10061.26. The mean peak height for He-rich spots corresponds to gas concentrations of the order of 3 cm^3 of ^4He per gram.

The averaged ^4He concentrations for each of seven grain size fractions and five mineral components of handpicked dust grains are shown in Fig. 2. Clearly, the He content decreases by a factor of about 10 from ilmenite to Ti-rich glass fragments, to pyroxene, and to plagioclase. It is also seen that He concentrations increase toward smaller grain sizes nearly linearly with the re-

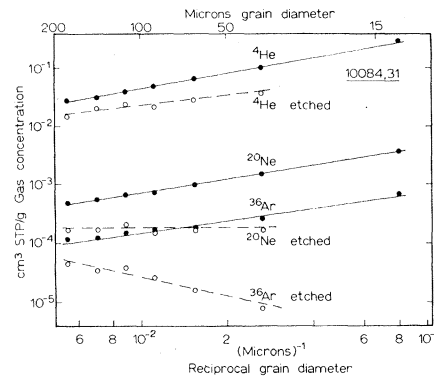
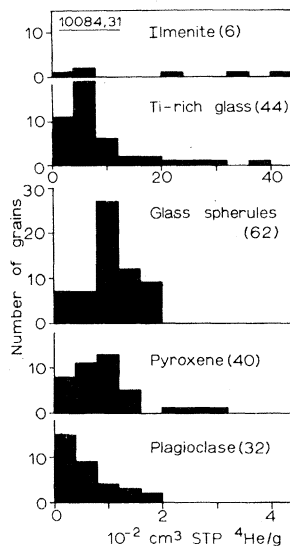


Fig. 3 (left). Fluctuation of ^4He concentration in individual grains of separated dust components $120 \pm 20 \mu\text{m}$ in diameter.

Fig. 4 (above). Concentrations of ^4He , ^{20}Ne , and ^{36}Ar plotted against reciprocal grain size diameter of unseparated lunar dust before and after etching.

Figure 2 also shows the He reduction due to etching of the outer 2 μm for the same five components and seven grain sizes. Amounts of He are generally lowered by factors of 2 to 10; nevertheless, even for etched minerals the relation between He and reciprocal diameter essentially remains.

The statistical distribution of He content in single grains of the same size is shown for each component in Fig. 3. The histogram applies to the $120 \pm 20 \mu\text{m}$ fraction; similar histograms were obtained for all other sieve fractions. Variations are large for each type but largest for the Ti-rich components.

Figure 4 shows the results of the measurements on sieve fractions of unseparated dust. The linearity between gas concentration and reciprocal diameter is valid for He as well as for Ne and Ar. Going from 90 μm to 13 μm radius, the $^4\text{He}/^{20}\text{Ne}$ ratio slightly increases, from 58 to 77. The same is true for the ratios $^{20}\text{Ne}/^{36}\text{Ar}$ (3.9 to 5.8) and $^4\text{He}/^{36}\text{Ar}$ (230 to 440). After etching these ratios increase, pronouncedly for smaller grain sizes. The isotopic ratio $^4\text{He}/^3\text{He}$ (2800), $^{22}\text{Ne}/^{21}\text{Ne}$ (32 to 23), $^{20}\text{Ne}/^{22}\text{Ne}$ (13.1 to 12.5), $^{36}\text{Ar}/^{38}\text{Ar}$ (5.4 to 5.2), and $^{36}\text{Ar}/^{40}\text{Ar}$ (1.0 to 0.6) decrease only very little with increasing grain size. Etching reduces $^4\text{He}/^3\text{He}$ by about 8 percent, $^{20}\text{Ne}/^{22}\text{Ne}$ by about 15 percent, and $^{22}\text{Ne}/^{21}\text{Ne}$ by a factor of about 2 for all grain sizes. The $^{38}\text{Ar}/^{36}\text{Ar}$ ratio in etched samples decreases with grain size down to 3.7 for the 25 to 50 μm fraction. The $^{40}\text{Ar}/^{36}\text{Ar}$

ratio increases after etching, especially for small grain sizes, where it reaches a maximum value of 6.6.

Scans across polished sections of the crystalline rock 10057.22 liberated less He than was detectable by our method, even with the beam intensity increased to 25 μA . Two other specimens (10057.80 and 10085.41) had pitted surfaces and were most likely exposed to the solar wind also. Many scans going from a freshly broken surface to the pitted surface clearly showed the rare gas implantation on the pitted surface (Fig. 5.) The quantity of He per square centimeter is $\sim 10^{-2}\text{cm}^3$. Repeated scans perpendicular to the pitted surface revealed an average thickness of $\sim 10\ \mu\text{m}$ for the He loaded layer (Fig. 5). Again, if ilmenite grains form the surface, the He concentrations are highest. For penetration depths of about $10\ \mu\text{m}$, an average ^4He concentration of $3\ \text{cm}^3$ per gram results.

The analysis of gases included in cavities of the crystalline rock 10057.22 gave the following results (in 10^{-8}cm^3): In a 56 mg piece, N_2 , 700; H_2 , 5; ^4He , 3; ^{40}Ar , 1.4; $^{40}\text{Ar}/^{36}\text{Ar} = 700$. In a 50 mg piece: ^4He , 0.7; ^{40}Ar , 0.63; H_2 and N_2 not detected. The Ar is clearly radiogenic, probably because of degassing after rock crystallization.

The foregoing results show that the rare gases consist of three components. The main contribution seems to come from trapped solar wind particles. There are also small radiogenic and spallogenic components.

A solar wind origin is suggested by the proportionality of the gas concentrations with the reciprocal diameter of the grains, both in mineral components and in unseparated sieve fractions. Since the concentrations increase with the surface to volume ratio, the gases must be concentrated in the outermost surface layers. This idea is supported by the composition of the gases, which agrees with the so-called solar abundances. All gas bearing grains must have been at the uppermost surface at one time or another. In a similar way, the surfaces of glass pitted crystalline rocks were loaded with gases while they were exposed to the sun, but the interior was always shielded. Since breccias are composed of dust and lithic fragments, it is natural that the matrix contains solar gases while they are undetectable in lithic fragments. Mineral grains without detectable gas content most likely were never exposed to the surface or were degassed at a later stage. The

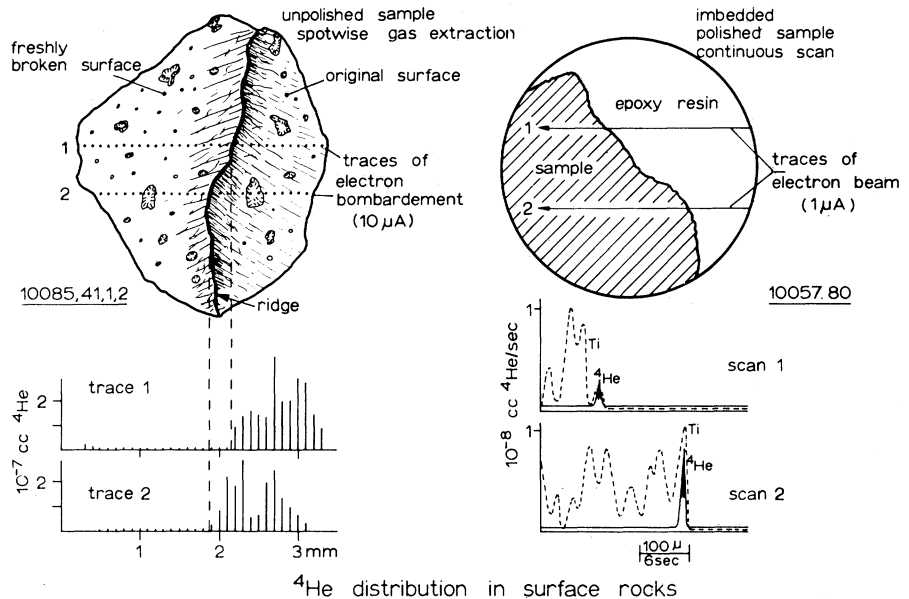


Fig. 5. Distribution of ^4He at the surface of crystalline rocks 10057.80 and 10085.41.

correlation of He with Ti and to some extent with Fe, Cr, and Mn and the anticorrelation between He and Ca may be explained by different diffusion constants or gas adsorption properties of different minerals. The fact that grains of the same mineral differ substantially in their gas concentration indicates different exposure times or partial outgassing.

The mean thickness b at which the gas of the surface is reduced by a factor of e can be calculated from a simple mathematical treatment. Assuming an exponential decrease of gas concentration toward the interior of the grains, it is possible to infer b from the measured degree of gas reduction due to etching; b is $10\ \mu\text{m}$ for He, $6\ \mu\text{m}$ for Ne, and $5\ \mu\text{m}$ for Ar. These different b values indicate that diffusion is responsible for the fact that b_{He} is larger than the mean penetration depths of solar wind He ($0.05\ \mu\text{m}$). The mean layer thickness b_{He} is in good agreement with the value directly measured at the surface of crystalline rocks (Fig. 5). Applying $b = 10\ \mu\text{m}$ to the He measurements, one ends up with the same surface concentration of $10^{-2}\ \text{cm}^3$ of ^4He per square centimeter as found before. This concentration is much smaller than the product of solar wind flux and exposure age, because of shielding and possibly surface saturation. For the smallest sieve fraction the apparent b_{Ar} value is smaller than for larger grain sizes. This is still unexplained; it may be that some particular mineral is enriched in the smallest fraction.

Stepwise heating experiments (3) yield an average diffusion constant for ^4He at 97°C in lunar dust of $D/a^2 \sim 3 \times 10^{-2}\ \text{sec}^{-1}$. A rough estimate for the time required to fill the interior of a $100\ \mu\text{m}$ grain yields $\sim 10^{3 \pm 1}$ years. Assuming a continuous turnover, the average exposure age of lunar surface material yields a rate of $\sim 1\ \text{m}$ per 100×10^6 years. This would correspond to a solar wind penetration time of $\sim 10^4$ years per $100\ \mu\text{m}$. More detailed diffusion experiments should be undertaken.

The location of the solar wind particles in the surface makes it easy to remove them together with the surface layer so that spallogenic and radiogenic components become relatively enriched in the remaining sample. The spallogenic component can clearly be distinguished from the $^{22}\text{Ne}/^{21}\text{Ne}$ and $^{36}\text{Ar}/^{38}\text{Ar}$ ratios in the etched dust fractions. Assuming a production rate of $0.15 \times 10^{-8}\ \text{cm}^3$ of ^{21}Ne per gram per 10^6 years gives an apparent exposure age of 500×10^6 years. An ^{38}Ar exposure age could be estimated only for the smallest sieve fraction. That age is also about 500×10^6 years. The apparent ^3He exposure age (200×10^6 years) is uncertain because of high ^4He content and possible diffusion losses. The ^{21}Ne and ^{38}Ar exposure ages are considered as upper limits, since spallogenic gases could be partially inherited.

The etched small grain size fractions show a pronounced enrichment of ^{40}Ar . Assuming an $^{40}\text{Ar}/^{36}\text{Ar}$ ratio of 1 in the solar wind, the radiogenic ^{40}Ar

content amounts to $\sim 4.2 \times 10^{-5} \text{cm}^3$ per gram of dust. If we assume an average K concentration of 1000 parts per million, a K-Ar age of 3.5×10^9 years results.

T. KIRSTEN
F. STEINBRUNN, J. ZÄHRINGER
Max-Planck-Institut für
Kernphysik, Heidelberg, Germany

References and Notes

1. Lunar Sample Preliminary Examination Team, *Science* **165**, 1211 (1969).
2. J. Zähringer, *Earth Planetary Sci. Lett.* **1**, 20 (1966).
3. O. A. Schaeffer *et al.*, private communication and *Science*, this issue.
4. We thank W. Gentner, A. Haidmann, P. Horn, E. Jessberger, H. W. Müller, H. Richter, D. Storzer, and H. Weber for their assistance in this work.

4 January 1970

100 g of bulk fines (10084,16), <1 mm size, was received on 12 September (52 days after lunar landing). The second sample, two chunks of rock 10017 (a coarse-grained rock of mass 980 g) was received on 3 October. Figure 1a shows a drawing of this rock, with an outline of the approximate position of the specimens. The rock had two plausible surface orientations; most photographs made in the preliminary examination were in what we now consider a position inverted relative to its orientation on the moon (5).

Samples were subjected to grinding (rock), magnetic separation (rock and dust), and leaching (dust). They were dissolved in HF-HNO₃, with carrier addition where appropriate, in a Teflon still under flowing N₂. Chlorine and Si were recovered in the distillate. The residue from the distillation was heated with H₂SO₄ in a Pt dish to remove HF; HCl was added, and Fe was extracted. The "main chemistry" was completed by anion- and cation-exchange column steps. This main chemistry was carried out, with variations, for two 50-g portions of soil and for six subdivisions of the rock (Fig. 1b). The resulting fractions, containing usually one element of interest, sometimes two or three, were purified chemically and radiochemically.

Chemical analyses for calculation of chemical yields and for following the progress of separations and recoveries were carried out by atomic absorption spectrometry. Agreement was good between these analyses and those available to us from others, with a few exceptions. In some cases the analytical data of others were used for final yield calculations. Overall yields were usually in

Pattern of Bombardment-Produced Radionuclides in Rock 10017 and in Lunar Soil

Abstract. A large number of radionuclides have been measured as a function of depth in lunar rock 10017 and in bulk fines. Data are reported on ¹⁰Be, ²²Na, ²⁶Al, ³⁶Cl, ⁴⁹V, ⁵³Mn, ⁵⁴Mn, ⁵⁵Fe, ⁵⁶Co, ⁵⁷Co, and ⁵⁹Ni and on upper limits for ⁴⁶Sc, ⁴⁸V, ⁵¹Cr, and ⁶⁰Co. The results for several nuclides show striking evidence of excess surface production attributable to solar flare particles. Data for short-lived species, ⁵⁶Co, ⁵⁷Co, ⁵⁴Mn, ⁵⁵Fe, and ²²Na, appear consistent with fluxes from known recent events. Long-lived species demonstrate the existence of solar flare protons and alphas at least for the last 10⁵ to 10⁶ years, at fluxes comparable to those now observed.

Measurements of the concentration of short- and long-lived radionuclides in meteorites have been useful in unraveling the history of the high-energy radiation which produced them and of the target objects (1, 2). Similar studies on lunar surface materials have the same potential usefulness, with some special advantages. A lunar sample has suffered no ablation, and in principle its recent orientation and depth are known. The planet which they sample is a single, intensely studied one at a known orbital position.

We attempted to study processes of gardening by impact or other processes on the lunar surface, through times of exposure and depth variations, and to

decipher the fossil record of solar and galactic high-energy particles in the earth-moon region. Since the longest half-lives available are less than 3×10^6 years, and since measured bombardment ages are generally much longer than this (3, 4), it appears that the samples so far received are, for our present purposes, relatively fixed targets. Thus we have generally concentrated on the objective of using the rock and soil samples to study the high-energy particle emission of the sun on a time scale up to millions of years. Nevertheless, a combination of radionuclide, rare gas, and track data can still give much information on turnover rates.

We received two lunar samples. First,

Table 1. Summary of counting results (dpm/kg). Limits (2 σ) in bulk fines sample: ⁷Be, 250; ⁴⁶Sc, 9; ⁴⁸V, 38; ⁵¹Cr, 45; and ⁶⁰Co, 5.

Nuclide	Half-life	Rock 10017					Bulk fines	
		T4DF (0 to 4 mm)	T4U (4 to 12 mm)	T4I (12 to 30 mm)	T3SI (60 mm)	Houston RCL*	This work	Houston RCL
¹⁰ Be	2.5×10^6 y		16 ± 2	16 ± 2			15.7 ± 1.6	
²² Na	2.6 y	76 ± 10	43 ± 6	37 ± 6			55 ± 7	51 ± 9
²⁶ Al	7.4×10^5 y	133 ± 15	70 ± 10	57 ± 9	31 ± 5	39 ± 7	108 ± 17	$120(\pm 19)$
³⁶ Cl	3×10^5 y	12 ± 5	16 ± 2	16 ± 2	63 ± 12	$73(\pm 13)$	17.0 ± 1.6	
⁴⁹ V	330 d						7.4 ± 2.0	
⁵³ Mn	$\sim 2 \times 10^6$ y	107 ± 21	45 ± 13	52 ± 10				
⁵⁴ Mn	303 d	33 ± 17	34 ± 22	10 ± 11		$34(\pm 13)$	18 ± 10	28 ± 9
⁵⁵ Mn and ⁵⁴ Mn			98 ± 15	88 ± 10			82 ± 11	
⁵⁵ Fe	2.6 y	420 ± 44	94 ± 27	93 ± 30	97 ± 24		195 ± 22	
⁵⁶ Co	77 d	125 ± 20	< 16	< 8		$26(\pm 6)$	44 ± 6	40 ± 10
⁵⁷ Co	270 d	5.6 ± 2.6	< 1.7	< 2.4			< 1.8	
⁵⁹ Ni	8×10^5 y		< 4				2.6 ± 0.8	

* Houston 10017 data were measured using the whole rock (14).